

## USE OF REMOTE SENSING DATA AND GIS TECHNOLOGY FOR ASSESSMENT OF LANDSLIDE HAZARDS IN SUSVA VALLEY, ITALY

*Nora Tassetti, Annamaria Bernardini and Eva Savina Malinverni*

DARDUS-Università Politecnica delle Marche, Ancona, Italy;  
{n.tassetti / a.bernardini / e.s.malinverni}@univpm.it

### ABSTRACT

The aim of the research was to monitor and assess landslide hazards by remote sensing data processing and GIS spatial analysis. The automatic classification of remote sensing images provides many useful land use information to combine in a GIS environment with other spatial factors influencing the occurrence of landslide.

The upper part of Susa Valley, in the Italian Western Alps, was chosen as test area because of a large variety of remote sensing data available by ISPRES WG VIII/2 with the aim to exchange information and experience in the field of geomatic techniques.

It is well known that the occurrence of landslides is controlled by a lot of morphological, geological, and human factors. We have chosen, regarding the available data, the following factors: acclivity, aspect, lithology, land use and precipitations. We have built up a mathematical predictive model enabling actual/potential unstable slopes. It is a linear model where the hazard score depends on instability factors and the coefficients are based on a statistical evaluation. The hazard score is classified into hazard rating to produce a landslide hazard assessment map in GIS environment. This model gives also indications about the relevant factors influencing slope instability. This tool makes the GIS a Spatial Decision Support System (SDSS) for land management.

**Keywords:** Landslides, Deep Seated Slope Gravitational Deformations, Spatial Decision Support System

### INTRODUCTION

The selected test area is related to the upper part of Susa Valley, Italian Western Alps, in the Piemonte Region (Figure 1). This area is subject to large slope instabilities and presents a very rough landscape with altitudes ranging between 700 and 3,500 m a.s.l. The geology, geomorphology, and land use are extremely heterogeneous.

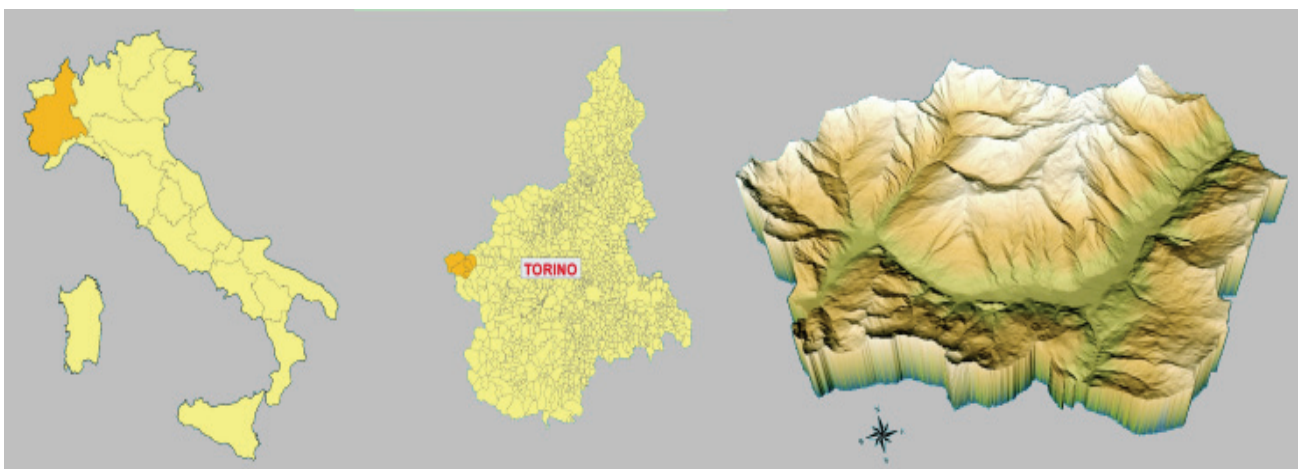


Figure 1: Location of the study area: Susa Valley in the North of Italy, Piemonte Region.

Many GIS-based analysis models and quantitative prediction models of landslide hazard have been proposed in the literature (1,2,3). The advantages in the use of GIS for assessing landslide hazards are the following:

- a much larger variety of hazard analysis techniques becomes attainable;
- it is possible to improve models by evaluating their results adjusting the input variables. Users can achieve maximum results by an iterative process of trial and error, whereas it is difficult to use these models even once in the conventional manner. Therefore, more accurate results can be expected.

The steps of this study were:

- Construction of a landslide inventory map. Data source has been acquired by the Web Geoportal ARPA Piemonte (IFFI Project);
- Identification of the physical factors, which are directly or indirectly correlated with slope instability (instability factors), and construction of thematic maps related to landslide affecting factors;
- Evaluation of contribution of each factor to landslide susceptibility by means of a bivariate statistical method;
- Production of the final landslide susceptibility map based on GIS techniques coming from the land surface classification according to different susceptibility degrees.

## LANDSLIDE INVENTORY MAP AND AFFECTING FACTORS MAPS

The landslide inventory is a fundamental prerequisite for landslide hazard analysis based on GIS. The landslide inventory covers about 207 km<sup>2</sup>, representing 62% of the whole area of study. The landslide observation dates or periods have been recorded since 2004, when the IFFI project started, so time information about the previous landslides are missing or are not accurate. For this reason, the time factor was not taken into account in the analysis. Figure 2 shows the distribution of landslides subdivided into different types. The prevalent type of landslide, DSSGD (Deep Seated Slope Gravitational Deformations), covers 36% of the study area but did not influence our analysis, because it depends on other instability factors not considered in this study.

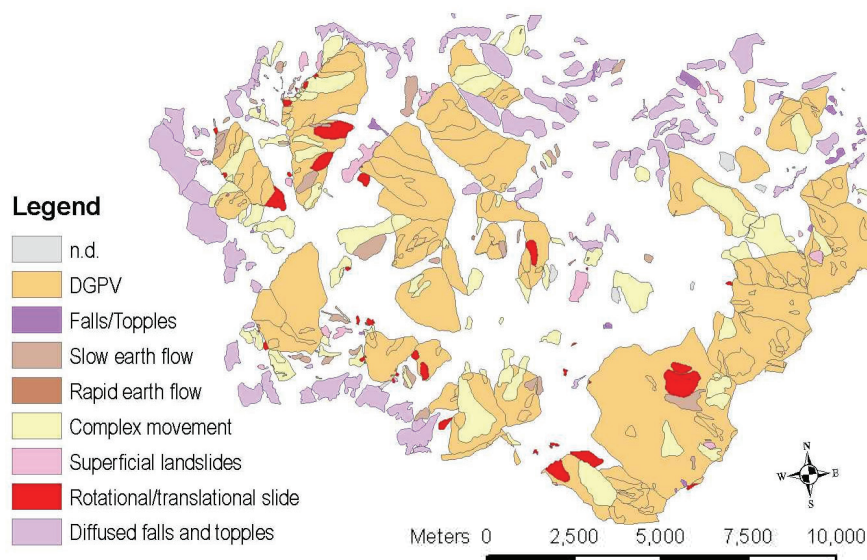


*Figure 2: Landslide inventory map.*

It is well known that many factors play an important role in generating slope-failure. Unfortunately, few of these can be acquired, mapped and used cost-effectively in landslide assessment over wide areas. In the present project, a set of five instability factors has been analyzed for correlation with landslide events according to studies published in the literature (3,4,5): geology; land use; slope;

aspect; precipitation. The GIS has been developed by means of ArcGIS™ ver. 9.1. The landslide occurrences and the instability factors have been recorded as vector data, re-classed, saved as separate layers in the database and then rasterised for the next analysis (Spatial Analyst Tool).

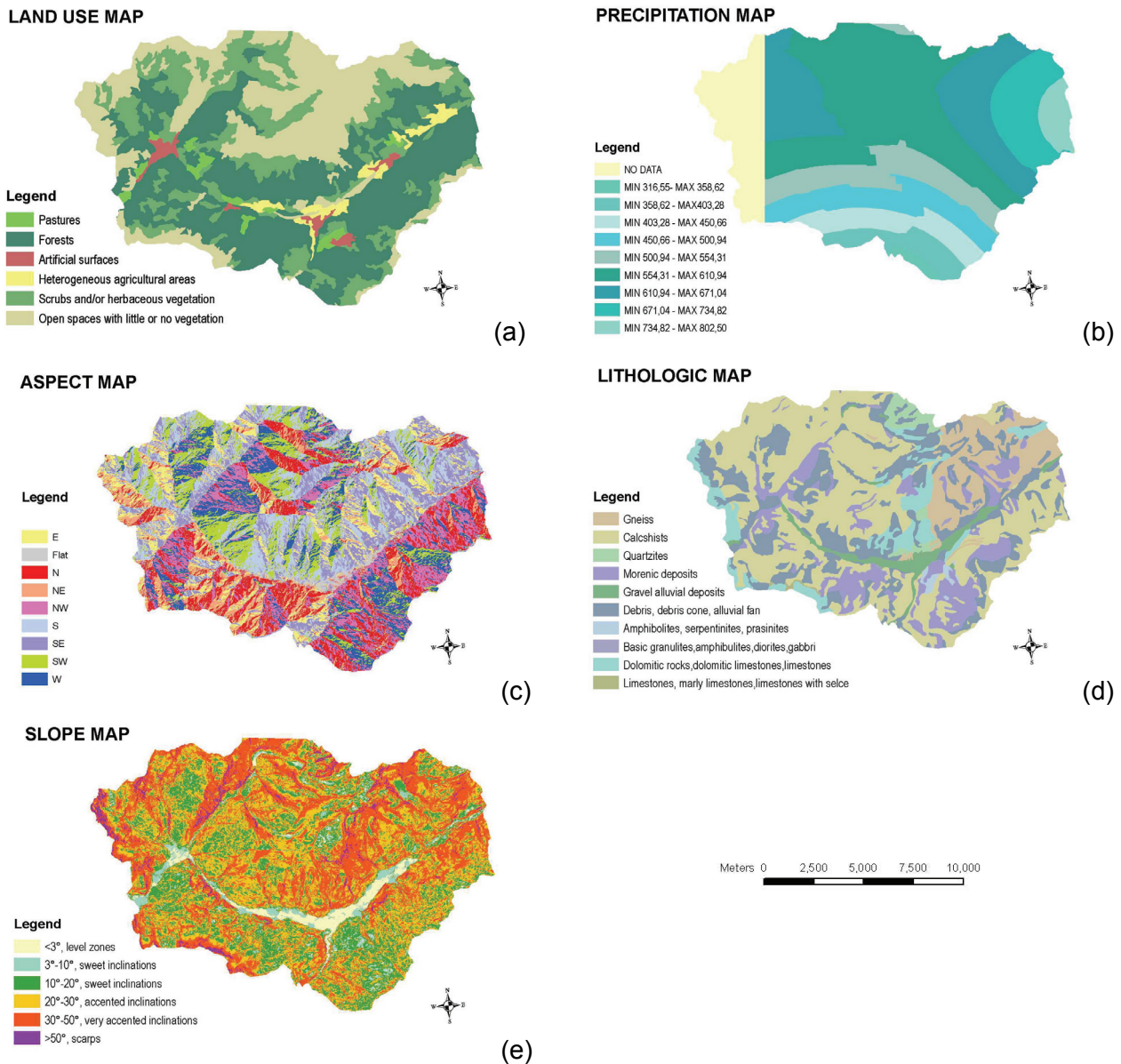


Figure 3: Affecting factors maps.

Geomorphology, such as Slope and Aspect, has been calculated by  $10 \times 10 \text{ m}^2$ . A Digital Elevation Model has been provided by ARPA Piemonte. The slope classes have been divided into six intervals with increasing criticality level (Figure 3e). Depending on regional climate, Aspect can marginally effect slow stability with south-facing slopes susceptible (Figure 3c).

The geological map is the result of a wider project (CARG Project, National Geological Survey) that will cover the whole country in the future. Susa Valley is mainly characterised by mixed incoherent deposits of glacial and post-glacial origin, calcschists and, subsequently, ophiolites; quartz and gneiss are less abundant. The geomorphology is dominated by glacial modelling, followed by recent river actions, mainly in the upper part of the valley. A new simplified lithology map has been prepared from the original geological map to simplify the following attribution of weights. The lithological formations have been classified upon their geotechnical characteristics into ten lithological groups (Figure 3d).

The Land Use Map has been created integrating European Corine 2000 Project data (provided by the courtesy of APAT and Piemonte Region) and information coming from other satellite image classification (Quickbird, Ikonos, Aster, Eros) provided by ISPRS. The land cover results have been re-classed into five groups considering the degree of soil permeability, the erosion susceptibility of the soil and the landslides. The herbaceous cover is characterised by high vulnerability, like shrubs or trees with scarce canopy cover (Figure 3a).

The Precipitation Map has been prepared from daily weather observations provided by ARPA of Piemonte Region. We used the Kriging method to estimate the unknown rainfall depth as weighted average of every neighbouring location value (6). Let  $l_1, l_2, \dots, l_n$  be the  $n$  meteorological stations with given precipitation value  $z(l_i)$  and  $x$  the generic unsample location,  $z(x)$  is estimated as:  $z(x) = \sum w_i \cdot z(l_i)$ . The weights  $w_i$  have been estimated by the semivariogram model, that captures the spatial dependence between samples by plotting semivariance as a function of reciprocal distance. Semivariance increases when the reciprocal distance increases, up to some given separation distance, from which points are unrelated. Every analysis has been computed by means of the Geostatistic Analyst Tool in ArcGIS™. The software calculates different models of semivariograms (isotropic or anisotropic). We preferred the anisotropy named Hole Effect Model, because it is characterised by a least root main square. The Hole Effect Model reflects pseudo-periodic or cyclic phenomena (7). In this case, the hole effect is related to the existence of mountains that exceed 3,000 m of altitude, with prevalent precipitations in the form of snow. In this study, we considered only rainfall precipitation, because the precipitation in the form of snow is not immediately correlated with landslide occurrence. Thus, the presence of these mountains creates two high-values in the rainfall field below the altitude of 1,500 m in NE-SW direction. Considering only the rainfall precipitations, an inverse correlation exists between the rainfall data and the altitude of the meteorological stations. We used also the terrain elevation as secondary variable incorporated in estimating precipitation. The Co-kriging Method produced an improvement in the model accuracy of about 20%. The mean annual precipitation is in a range of 250-800 mm and has been grouped into ten classes (Figure 3b). The highest rainfall estimated values have been observed in the North of the study area and the lowest ones in the South.

## LANDSLIDE SUSCEPTIBILITY

Many efforts in the hazard zonation research have been made in the past 30 years, as a consequence of the urgent demand for slope instability hazard mapping. Different methods can be applied in order to rank slope-instability factors. They assign different hazard levels to the mapping units of the region to be investigated (8). We can distinguish direct or indirect methods. Direct methods essentially consist of the geomorphological mapping. Among the indirect methods, the heuristic (index) and the statistical approaches have been more frequently applied in mapping hazard over wide regions with the aid of GIS related techniques. In the heuristic approach, instability factors are ranked and weighted according to their assumed or expected importance in causing mass-movement. The statistical approach is based on the observed relationships between each factor and the past and present landslide distribution. Among the commonly used GIS analysis models for landslide hazard, Certainty Factors (CF) have been experimentally investigated (9,3). The CF, defined as a function of probability (1), was originally proposed by Shortliffe and Buchanan (10) and later modified by Heckerman (11):

$$CF = \begin{cases} \frac{pp_a - pp_s}{pp_a(1 - pp_s)} & \text{if } pp_a \geq pp_s \\ \frac{pp_a - pp_s}{pp_s(1 - pp_a)} & \text{if } pp_a < pp_s \end{cases} \quad (1)$$

where  $pp_a$  is the conditional probability of a number of landslide events occurring in class  $a$  and  $pp_s$  is the prior probability of the total number of landslide events occurring in the study area. The CF value varies between -1 and 1, a positive value means an increasing certainty in landslide occurrence, while a negative value corresponds to a decreasing certainty.

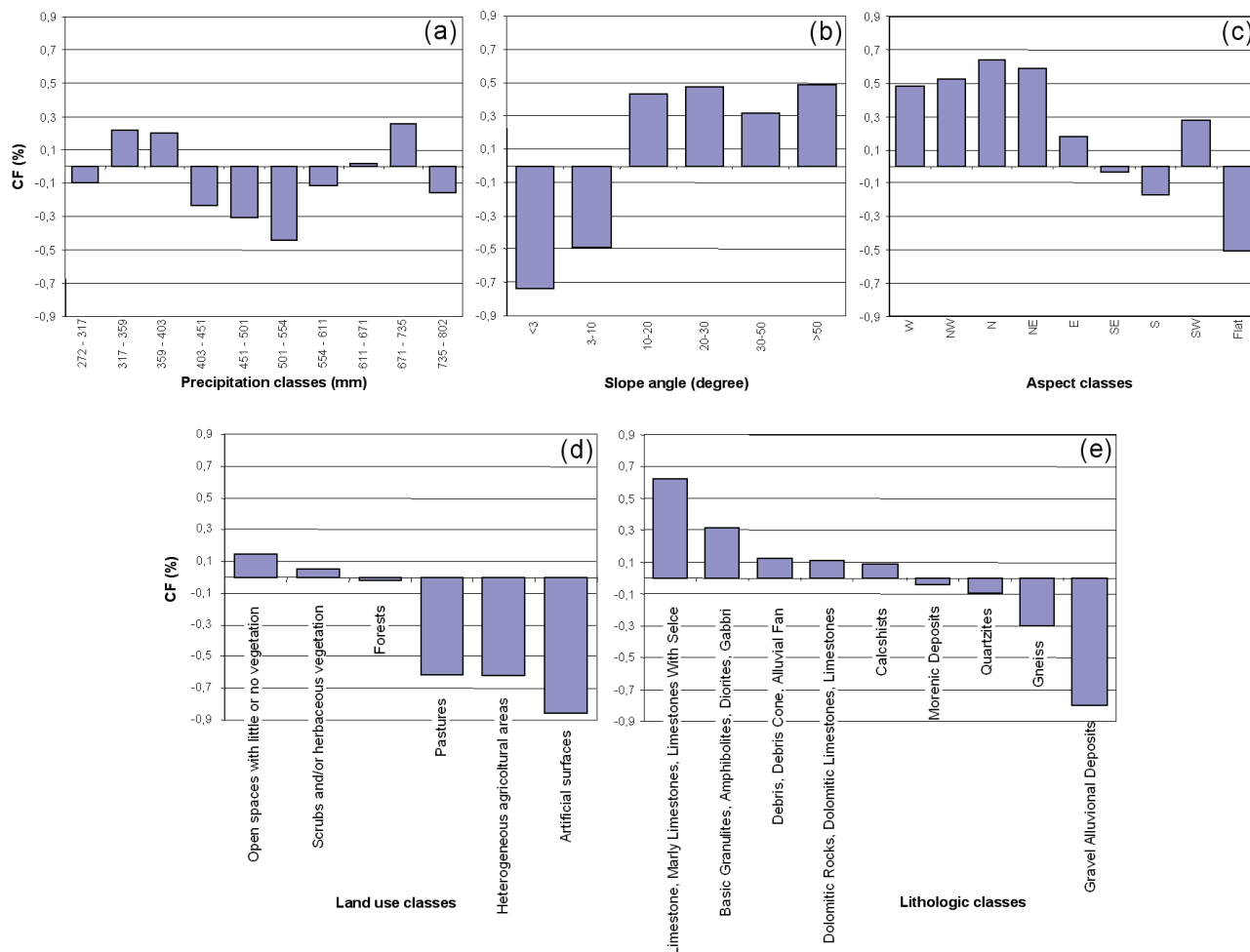


Figure 4: CF value for each instability factor. The classes with high CF value have high landslide susceptibility.

The favourability values ( $pp_a$ ,  $pp_s$ ) have been derived by overlaying each data layer with the landslide inventory layer in ArcGIS™ and calculating the landslide occurrence frequency. CF values have then been calculated for each class in each affecting factor (Figure 4). Morphology is shown to be the major controlling factor for land sliding. In particular:

**Slope Angle:** the 95% of slopes in the Susa Valley are characterised by a value of slope angles between 10-50%. The CF values of slopes are negative when the slope angle is lower than 10% (Figure 4b). Calculating CF values for different typologies of landslide we obtained different values. In particular we observed that:

- for slope angles lower than 10%, the CF value remains always negative;
- for slope angles higher than 30%, the CF value is positive only for falls, topples and for widespread landslides. For rapid flow, the 30-50 slope class has the higher CF factor.

**Aspect factor:** Approximately 40% of the slopes are localised in surfaces with aspect N, N-E, N-W. In fact, these classes have values of CF higher than 0.5 (Figure 4c). The influence of aspect on the occurrence of landslides can be direct or indirect: direct, because the aspect influences the amount of water absorbed by soil or evaporated; indirect, because a correlation could be found between other landslide factors and the aspect factor (i.e. land cover, in particular regarding the presence of vegetation, geological structures, ...). Thus, the high correlation of landslides with the aspect factor can depend on the particular geological structure that could be investigated.

**Lithology factor:** The three classes (limestone, granulites and amphibolites) have a very little extension, so the results are not well founded. The highest value of CF corresponds to the debris, the smallest one corresponds to gravel alluvial deposits which are localised in flat areas (Figure 4e).

*Land Use factor:* The only class that gives a meaningful contribution to the landslide contains open spaces with little or no vegetation (Figure 4d).

*Precipitation classes:* In a range of 1 to 10 they represent the growing values of daily rainfall between 250 to 800 millimetres. The relation between rainfall and landslide did not seem meaningful. *CF* values have also been calculated for different typologies of landslide, but the results always showed an apparently casual distribution without correlation. The reason of the absence of correlation could be the relatively short period of observation (ten years) (Figure 4a).

*The database obtained* by overlaying each data layer with the landslide inventory layer, contains the information relative to the landslide type. We have analysed *CF* values relative to each landslide type, with two types of results: Correlation similar to this obtained by the total landslide area; no correlation depending of the reduction of samples. So we chose to use only one model for the susceptibility assessment.

### SUSCEPTIBILITY MAP

The overall estimation of the landslide susceptibility for an area results from the combination of the susceptibility levels of the individual factors. In particular, the maps have been first re-classed according to the *CF* value; then the data layers have been combined using the *CF* integration rule in ArcGIS™ (Raster Calculator Tool – Spatial Analyst).

Table 1: Susceptibility Classification by *CF* value (3).

Code	Range	Description	Hazard class
1	-1, -0.5	Very low certainty of landslide occurrence	High stability
2	-0.5, -0.05	Low certainty of landslide occurrence	Medium stability
3	-0.05, 0.05	Uncertainty. <i>CF</i> value within the range close to zero represent the interval in which no landsliding certainty can be expressed	Uncertainty
4	0.05, 0.3	Low certainty of landslide occurrence	Low instability
5	0.3, 0.8	Medium certainty of landslide occurrence	Medium instability
6	0.8, 1.0	High certainty of landslide occurrence	High instability

The integrated *CF* values have been classified into six hazard classes on the base of the threshold criterion in accordance with the methodology proposed by Lan et al. (3) as shown in Table 1. According to this criterion, we produced the final map reclassifying the areas by means of these six different landslide susceptibility levels (Figure 5a). Finally, the active landslide map was superimposed on the layer of re-classed *CF* value (Susceptibility Class). In Figure 5b, we compare the frequency of each susceptibility class (normalised on the whole study area) with the frequency of landslide in each susceptibility class, normalised on the whole landslide area.

We can observe that most landslides happen in the low susceptibility class. Ashis K. Saha et al. (12) propose a different approach for the choice of class boundaries. Referring to this methodology, *CF* values have been segmented into five distinct classes with boundaries fixed at  $(\mu - 1.5\sigma)$ ,  $(\mu - 0.5\sigma)$ ,  $(\mu + 0.5\sigma)$  and  $(\mu + 1.5\sigma)$ , where  $\mu$  and  $\sigma$  are the mean and the standard error of the distribution curve of *CF* value.

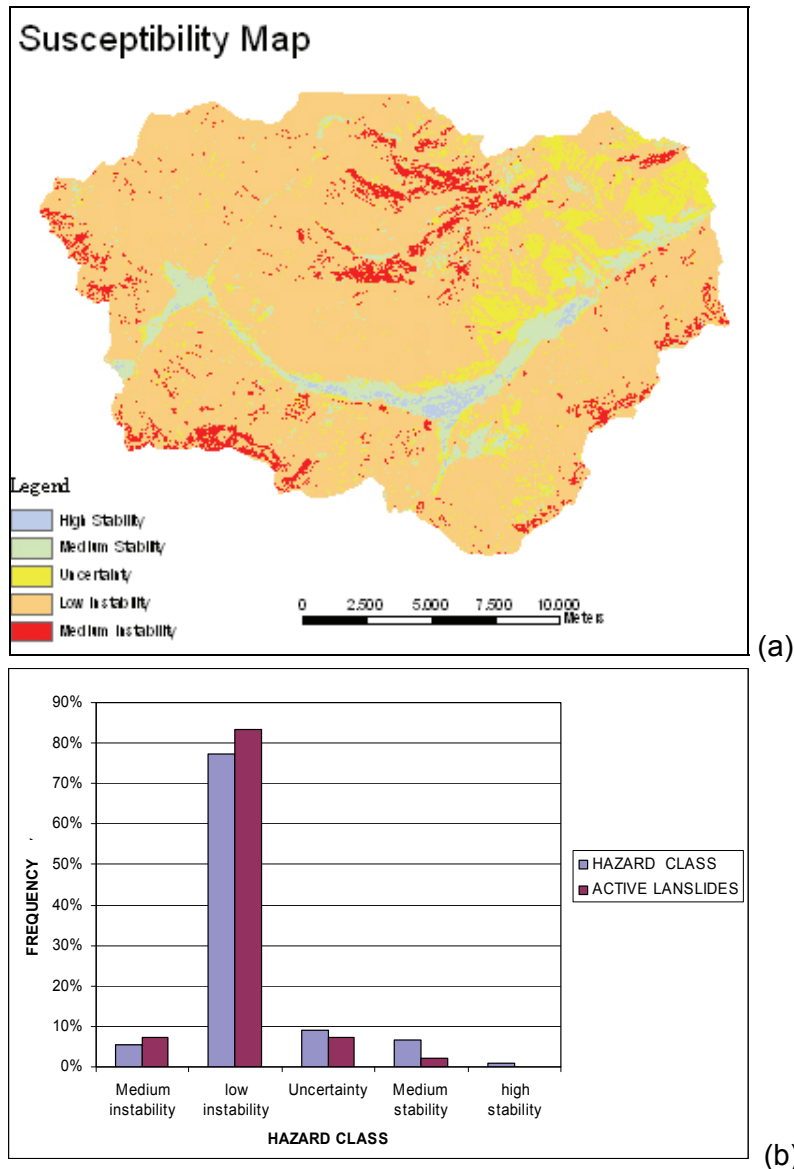


Figure 5: a) Landslide susceptibility map segmented by threshold criteria; b) Results overlaying the susceptibility map with the landslide map.

The second classification seems to perform better, with 28% of the area in a medium level of instability (Figure 6a) and 35% of landslides in the medium susceptibility class (Figure 6b).

In the instability map, the largest part of the territory is characterised by a low level of instability. The most critical area is an ecosystem characterised by steep slopes, bare soils on weathered substrata. In the land use map, the highest level of criticality is concentrated in the areas near the rivers, in the rangelands and in the ski slopes, frequently involved in erosion processes strictly connected with human activities. The relatively high frequency of landslides in class 2 (low instability) underlines the necessity of much more information to assess the landslide susceptibility and a major control during the data collection and processing (Figure 6b). The analysis has provided information on the susceptibility of the terrain to slope failures and can be used for the soil loss estimation, the localisation of new building sites and for the disaster management planning. The model can be applied to other mountainous areas with similar environmental characteristics, although a general and more accurate use needs more accurate landslide inventory, more damage data and more detailed information about the instability factors.

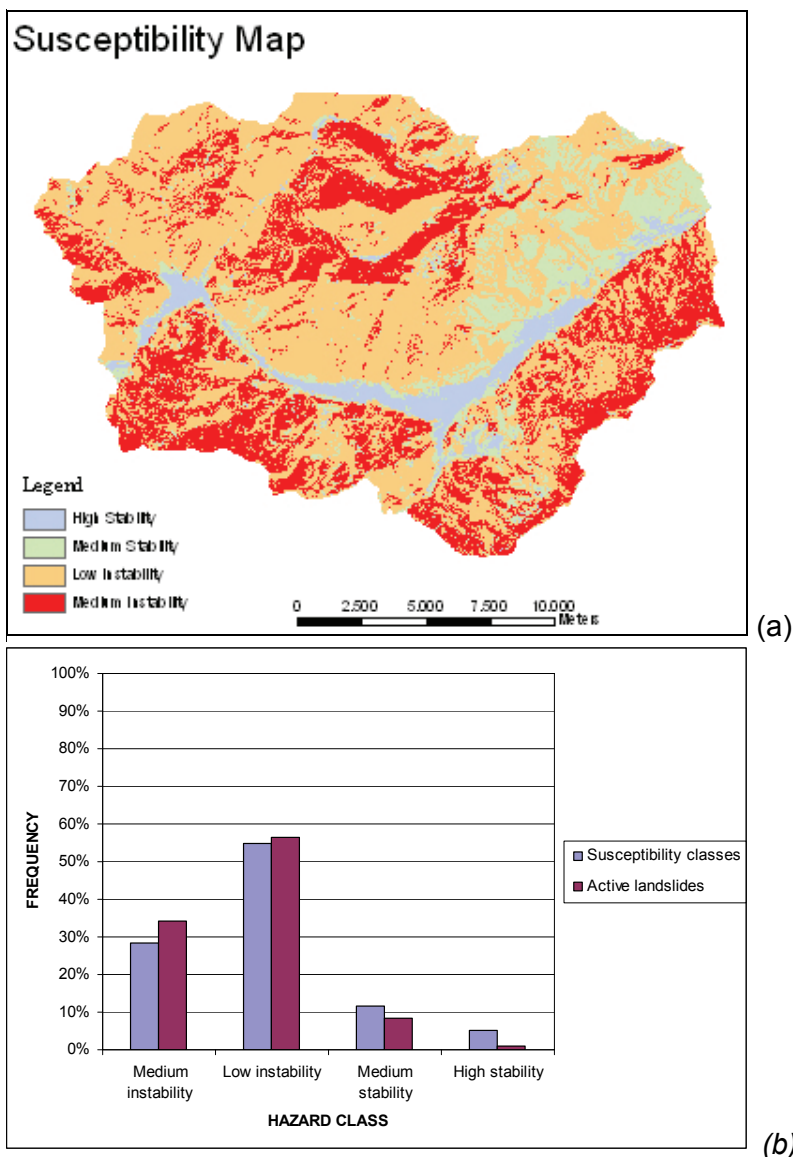


Figure 6: a) Landslide susceptibility map segmented by statistical analysis of the distribution of values; b) Results overlaying the susceptibility map with the landslide map.

**ACKNOWLEDGEMENTS**

Thanks a lot for the help provided by: ISPRS; Forlati, Giacomelli, Tiranti (ARPA Piemonte Region); Proff. P. Vivalda and T. Nanni (Univ. Politecnica Marche); we are grateful to S. Cascione for the collaboration during her degree thesis.

**REFERENCES**

- 1 Van Westen C J, 1994. GIS in landslide hazard zonation: a review with examples from the Colombian Andes. In: Mountain Environment and GIS, edited by M F Price & D I Keywood (London: Taylor and Francis) 35-65
- 2 Carrara A & F Guzzetti, 1999. Use of GIS technology in the prediction and monitoring of landslide hazard. Natural Hazards, 20: 117-135

- 3 Lan H X, C H Zhou, L J Wang, H Y Zhang & R H Li, 2004. Landslide hazard spatial analysis and prediction using GIS in the Xiaojiang watershed, Yunnan, China. Engineering Geology, 76: 109-128
- 4 Suzen M L & V Doyuran, 2004. Data driven bivariate landslide susceptibility assessment using geographical information systems: a method and application to Asarsuyu catchment, Turkey. Engineering Geology, 71: 303-321
- 5 Zezere J L, 2002. Landslide susceptibility assessment considering landslide typology. A case study in the area north of Lisbon (Portugal). *Natural Hazards and Earth System Sciences*, 2(1-2), European Geophysical Society, 73-82
- 6 Phillips D L, J Dolph & D Marks, 1992. A comparison of geostatistical procedures for spatial analysis of precipitations in mountainous terrain. Agricultural and Forest Meteorology, 58: 119-141
- 7 Journel A G & C J Huijbregts, 1978. Mining Geostatistics (New York: Academic Press) 600 pp.
- 8 Hansen A, 1984. Landslide hazard analysis. In: *Slope Instability*, edited by D Brunnsden & D B Prior (New York: Wiley) 523-602
- 9 Binaghi E, L Luzi & P Madella, 1998. Slope instability zonation: a comparison between certainty factor and fuzzy Dempster-Shafer approaches. Natural Hazards, 17: 77-97
- 10 Shortliffe E H & G G Buchanan, 1975. A model of inexact reasoning in medicine. Mathematical Biosciences, 23: 351-379
- 11 Heckerman D, 1986. Probabilistic interpretation of MYCIN's certainty factors. In: Uncertainty in Artificial Intelligence, edited by L N Kanal & J F Lemmer (New York: Elsevier) 298-311
- 12 Saha A K, R P Gupta, I Sarkar, M K Arora & E Csaplovics, 2005. An approach for GIS-based statistical landslide susceptibility zonation with a case study in the Himalayas, *Landslides*, 2: 61-69